Title

Aire mediates tolerance to insulin through thymic trimming of high-affinity T cell clones.

Journal

Proceedings of the National Academy of Sciences, 121(20)

Authors

Smith, Jennifer
Yuen, Benjamin
Purtha, Whitney
et al.

Publication Date

2024-05-14

DOI

10.1073/pnas.2320268121

Peer reviewed

PNAS RESEARCH ARTICLE | IMMUNOLOGY AND INFLAMMATION

Aire mediates tolerance to insulin through thymic trimming of high-affinity T cell clones

Jennifer A. Smith[a,1], Benjamin T. K. Yuen[a,1], Whitney Purtha[a], Jared M. Balolong[a], Jonah D. Phipps[a], Frances Crawford[b], Jeffrey A. Bluestone[c], John W. Kappler[b,d,e], and Mark S. Anderson[a,2]

Edited by Kristin Hogquist, University of Minnesota Medical School Twin Cities, Minneapolis, MN; received November 27, 2023; accepted March 16, 2024

Insulin is a central autoantigen in the pathogenesis of T1D, and thymic epithelial cell expression of insulin under the control of the Autoimmune Regulator (*Aire*) is thought to be a key component of maintaining tolerance to insulin. In spite of this general working model, direct detection of this thymic selection on insulin-specific T cells has been somewhat elusive. Here, we used a combination of highly sensitive T cell receptor transgenic models for detecting thymic selection and sorting and sequencing of Insulin-specific CD4+ T cells from Aire-deficient mice as a strategy to further define their selection. This analysis revealed a number of unique t cell receptor (TCR) clones in Aire-deficient hosts with high affinity for insulin/major histocompatibility complex (MHC) ligands. We then modeled the thymic selection of one of these clones in Aire-deficient versus wild-type hosts and found that this model clone could escape thymic negative selection in the absence of thymic Aire. Together, these results suggest that thymic expression of insulin plays a key role in trimming and removing high-affinity insulin-specific T cells from the repertoire to help promote tolerance.

Aire | insulin | antigen-specific | T cell selection | thymic selection

Significance

Insulin plays a crucial role in the autoimmune progression of type 1 diabetes, as evidenced by the simultaneous presence of autoantibodies and autoreactive T cells specific to insulin during the onset of the disease. Central tolerance in the thymus, achieved through promiscuous expression of insulin in thymic epithelial cells, is a crucial mechanism preventing the generation of these T cells. Robust measurements of thymic selection, employing T cell receptor transgenics, reveal that thymus Aire does not influence model register-3A and register-3B T cells. Importantly, our findings indicate that high-affinity insulin-specific T cells are deleted in an Aire-dependent manner within the thymus. Consequently, we propose a model in which Aire facilitates the deletion and selection of high-affinity insulin-specific T cells.

Thymic tolerance plays a key role in the prevention of autoimmunity. Autoreactive T cells are involved in the initiation of type 1 diabetes (T1D) disease state and its progression and are thought to arise at least in part due to the breakdown in thymic tolerance (1, 2). Insulin serves as a major target and stimulus for autoreactive cells, with insulin-reactive $CD4^+$ T cells and insulin-specific autoantibodies found in patients with T1D and in the nonobese diabetic (NOD) mouse model of T1D (3, 4). A number of elegant mouse experiments demonstrated that genetic deletion of the *Insulin* (*Ins*) genes results in complete protection against the development of autoimmune diabetes, underscoring the importance of insulin as a major epitope (5). Thus, understanding how immune tolerance against insulin is shaped is key to unlocking the pathogenesis of T1D.

Genetic studies of T1D and rare monogenic forms of T1D point to thymic expression of insulin as an important step in maintaining immune tolerance against pancreatic islet cells (6–8). Genetic studies have shown a strong association between allelic polymorphisms in the variable number of tandem repeats (VNTRs) region of the *Ins* gene promoter and to susceptibility to T1D (7, 9). Later studies went on to demonstrate that these polymorphisms correlate with *Ins* expression within the thymus. Individuals with low copy number *Ins*-VNTRs have low thymic *Ins* transcription and increased T1D incidence, while those with high copy number *Ins*-VNTRs have increased thymic *Ins* expression and lower disease propensity (7–11). We have also now come to appreciate that a key mediator of thymic expression of many self-antigens, including insulin, is the Autoimmune Regulator (*Aire*) (12). *AIRE* was originally identified as the defective gene in the rare monogenic autoimmune syndrome, Autoimmune Polyglandular Syndrome Type 1, which is characterized by the development of multiple autoimmune organ-specific manifestations including T1D (13–17). Aire is highly expressed in medullary thymic epithelial cells (mTECs) where it promotes the expression of many self-antigens, including insulin (18–20) and recent single-cell data in the human thymus has identified and mapped thymic *Ins* transcripts specifically to *Aire*-expressing cells (21). Thus, a more refined picture is emerging linking T1D susceptibility to thymic tolerance to insulin, implicating mTECs as key mediators in this process.

Despite the strong link of mTEC expression of *Ins* to T1D susceptibility, its direct impact on thymic selection against insulin-specific T cells remains unclear. Insulin-specific T cells have been detected in both T1D patients and NOD mice, suggesting that thymic deletion of such clones is not complete (5, 22–28). In the NOD mouse model, most identified insulin-reactive $CD4^+$ T cell clones are restricted to the 9 to 23 amino acid sequence of the B chain of insulin (InsB:9-23) (25, 26, 29, 30). Because this antigenic

The authors declare no competing interest.

This article is a PNAS Direct Submission.

[1]J.A.S. and B.T.K.Y. contributed equally to this work.

[2]To whom correspondence may be addressed. Email: Mark.Anderson@ucsf.edu.

This article contains supporting information online at https://www.pnas.org/lookup/suppl/doi:10.1073/pnas.2320268121/-/DCSupplemental.

Published May 6, 2024.

peptide is longer than the 9 amino acid binding pocket of the NOD MHC class II allele I-A^{g7}, how this peptide is arranged in the peptide binding pocket has been an area of deep investigation. Previously, three registers of InsB:9-23 have been characterized for binding in the nine amino acid groove of I-A^{g7}, register 1(12-20, Reg1), register 2 (13-21, Reg2), and register 3 (14-22, Reg3) (Fig. 1*A*). The register three arrangement of InsB:9-23 has an unfavorable binding affinity for the I-A^{g7} binding pocket because of the arginine I residue in the p9 position of the peptide, yet the vast majority of identified InsB:9-23 clones respond to the insulin peptide in this register. By mutating arginine (R) to glutamic acid (E) at p9 (Fig. 1*B*), the unfavorable arginine (due to its positive charge) is replaced with an optimal (negative, acidic) and improves peptide binding to the MHCII I-A^{g7} by 100-fold (31–33). This mimotope sequence is termed register 3A (Reg3A), and this peptide can be used as an antigen or in I-A^{g7} tetramers to characterize a large fraction of InsB:9-23 specific CD4^{+} T cell clones that have been derived from NOD mice. Additionally, a second mutation introducing glycine (G) into the P8 position, replacing the glutamic acid (E) of the peptide) termed register 3B (Reg3B) alters the side chain that interacts with TCRs. This peptide or I-A^{g7} tetramers with this peptide identify a distinct fraction of InsB:9-23 T cell clones that were also derived from NOD mice (33). Thus, the majority of InsB:9-23 T cells that have been cloned to date can be characterized as Reg3A or Reg3B. In parallel, work from the Unanue group has proposed a slightly different

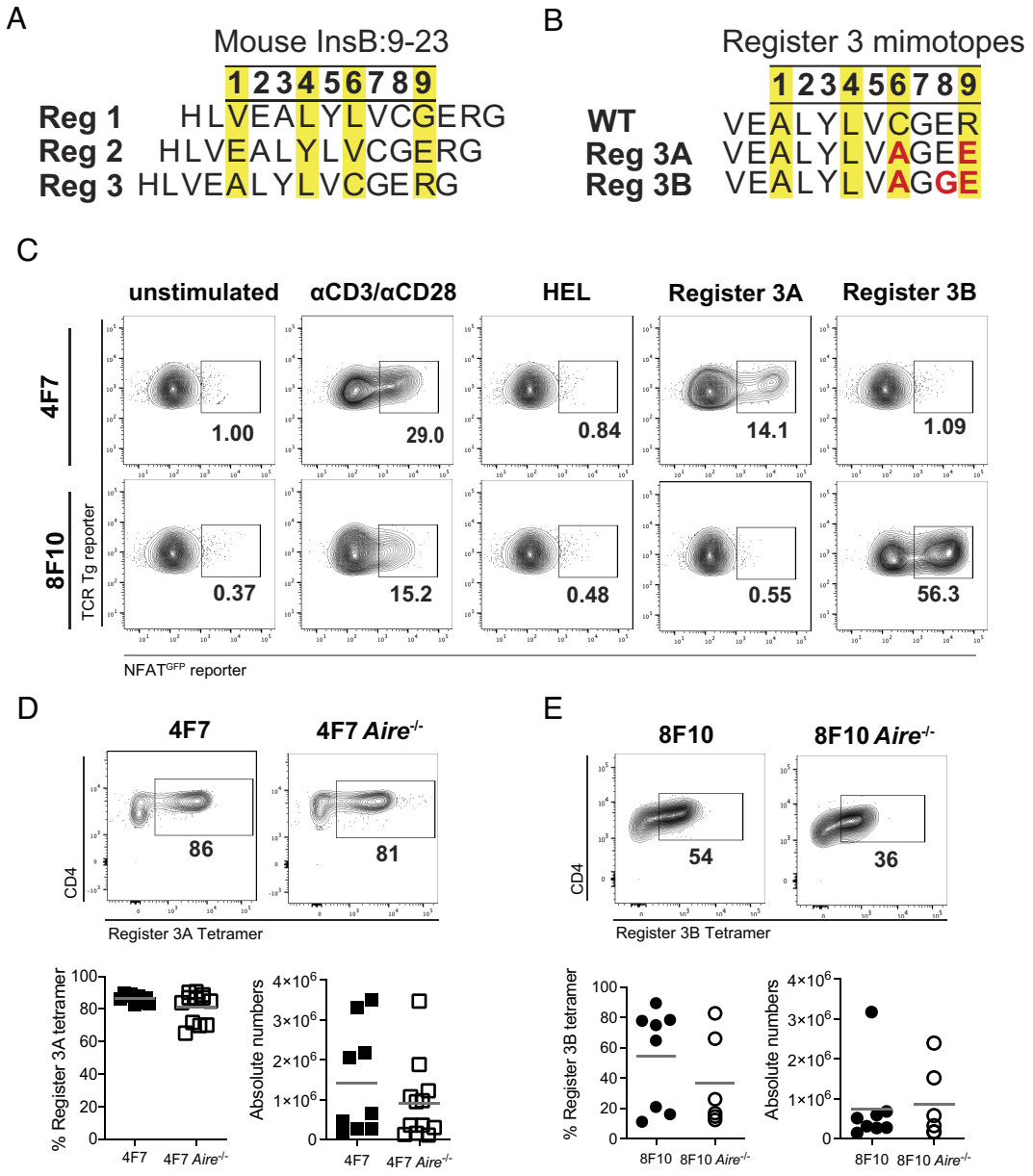

Fig. 1. Insulin-specific TCRs 4F7 and 8F10 are not dependent on Aire-expression in the thymus. (*A*) The immunogenic InsB:9-23 peptide can be bound in three distinct registers; the image illustrates how they sit with positions p1 to p9 (yellow highlight amino acids sidechains that would sit within the I-A^{g7} groove). (*B*) Insulin register three WT and mimotopes Reg3A and Reg3B. The mutations in the register three bound mimotopes are highlighted in red: p6C>A to prevent dimerization, p8E>G to improve Type B TCR interaction, and p9R>E to allow I-A^{g7} binding in register 3. (*C*) The 4F7 and 8F10 TCRs were cloned into the pMSCV-IRES-mCherry retroviral vector and transduced the TCR-deficient 58a^{-}b^{-} hybridoma cell line containing an NFAT-GFP reporter. Hybridomas were stimulated overnight with plate-bound HEL-tetramer and anti-CD3 and anti-CD28 antibodies as controls, and Reg3A and Reg3B-tetramer and their NFAT^{GFP} expression were assessed via flow cytometry. (*D*) Representative flow plots from the thymus of 4F7 TCR transgenic mice (8 to 12 wk old; male and female, n = 3 to 12). Pregated on CD4^{+}CD8^{-} TCRVβ2^{+} (4F7). The frequency of register 3A tetramer+ CD4 T cells, along with absolute numbers, is shown below. (*E*) Representative flow plots from the thymus 8F10 TCR transgenic mice (8 to 12-wk-old mice; male and female, n = 3 to 12). Pregated CD4^{+}CD8^{-} TCRVβ8.1/8.2^{+} (8F10) cells. The frequency of register 3B tetramer^{+} CD4 T cells, along with absolute numbers, is shown below.

nomenclature and peptide binding property for these clones, which is termed Type A and Type B (34). In previous work, Reg3A reagents have been shown to map to Type A cells, and Reg3B reagents map to Type B cells in this model (33).

Previous work on studying the behavior of Reg3A and Reg3B-specific T cells in the periphery of NOD mice has suggested that thymic expression of insulin influences the selection of Reg3A cells but that Reg3B cells can escape this selection (35, 36). A major limitation to this conclusion was lack of direct examination of these cell types in the thymus for their selection. Here, we tested Reg3A and Reg3B insulin-specific clones in a TCR-transgenic mouse system and found little influence for Aire-dependent thymic insulin expression on their selection (36, 37). We then expanded our analysis by sorting insulin-tetramer reactive cells from wild-type, *Aire*-deficient, and *Ins*-deficient genotypes and utilizing a single-cell sequencing approach to identify individual TCRs. We found evidence that in the *Aire*-deficient genotype, T cell clones with a high affinity for insulin were influenced by *Aire* for negative selection in both retrogenic and transgenic mouse models. Intriguingly, these types of high-affinity T cells tolerated a number of c-terminal mutations in the antigenic insulin peptide. Taken together, these results support a model whereby thymic expression of *Ins* plays a role in the thymic deletion of high-affinity T cell clones with specificity to insulin rather than previously proposed models for Reg3A (Type A) clones being dependent on *Aire* for thymic selection (35, 36, 38, 39).

Results

Aire Does Not Regulate the Negative Selection of Canonical Register 3A and 3B Insulin-Specific T Cells. To address the question of whether *Aire* regulates negative selection of canonical Reg3A and Reg3B insulin-specific T cells differentially, we examined two canonical insulin-specific T cell clones 4F7 and 8F10, characterized by the Unanue group as Type A and Type B, respectively (31, 33). Both TCRs utilize the TCR alpha chain TRAV5D-4 region but with unique CDR3 elements and have distinct TCR beta chains. To confirm the recognition of the InsB:9-23 peptide presented in Reg3, we utilized an in vitro retroviral expression system. TCR expression vectors were retrovirally transduced into $58\alpha^{-}\beta^{-}$ hybridoma lines containing a nuclear factor of activated T cells (NFAT)-inducible GFP reporter with CD4, incubated with plate-bound tetramers consisting of I-A^{g7} bound to Reg3A or Reg3B mimotopes, and analyzed for NFAT signaling via GFP expression. The 4F7-TCR signaled only to immobilized register 3A-tetramer while 8F10-TCR responded only to immobilized register 3B tetramer, confirming that 4F7 is a canonical register 3A/Type A clone while 8F10 is a canonical register 3B/Type B, insulin-specific T cell clone (Fig. 1*C*).

To assess these clones for thymic selection in the absence of *Aire* expression, we generated TCR transgenic mouse lines for both the 4F7 and 8F10 TCRs in the NOD background and crossed them onto the $Aire^{-/-}$ background (35, 37). TCR beta chain-specific antibodies and register3 mimotope I-A^{g7} tetramers were used to identify T cells expressing the transgenic TCRs. In $4F7^{Tg}$ (*Aire* sufficient) mice, $4F7^{Tg}$ ($Vb10^{+}$ register 3A-tetramer^{+}) $CD4^{+}$ T cells comprised more than 86% of the $CD4^{+}$ compartment in the thymus. When crossed to the $Aire^{-/-}$ genotype ($4F7^{Tg}$ $Aire^{-/-}$), there was no significant change in the frequency or absolute cell count of $4F7^{Tg}$ $CD4^{+}$ T cells in the thymus (81%) or in the spleen (24% versus 31%) (Fig. 1*D* and *SI Appendix*, Fig. S1*A*). The $4F7^{Tg}$ and $4F7^{Tg}Aire^{-/-}$ mice were also tracked for T1D incidence, and no differences were observed (*SI Appendix*, Fig. S1*B*). In addition, no differences were found in the frequencies or numbers of $Vb10^{+}$ regulatory T cell (Treg) ($CD25^{hi}$ $FoxP3^{+}$) within both the thymus and spleen (*SI Appendix*, Fig. S1*C*). Similarly, we did not observe a difference in the frequency or numbers of $8F10^{Tg}$ ($Vb8.3/8.2^{+}$ register 3B-tetramer^{+}) $CD4^{+}$ T cells in the thymus or the spleen between the $8F10^{Tg}$ and $8F10^{Tg}Aire^{-/-}$ mice (Fig. 1*E* and *SI Appendix*, Fig. S1*D*). These results showed that neither of these single canonical Reg3A nor Reg3B insulin-specific T cell clones was dependent on thymic *Aire* for selection.

Identification of _Aire_- or _Ins_-Dependent Insulin-Specific TCRs. Given that *Aire* expression had no impact on the thymic selection of Reg3A and Reg3B insulin-specific T cell clones, we hypothesized that this might be because both clones originated from an *Aire*-sufficient NOD mouse and that *Aire*-driven insulin expression in the thymus might induce negative selection of other clonotypes with, for example, higher affinity for insulin/I-A^{g7}. Thus, to better assess the potential impact of *Aire* on the selection of the full endogenous repertoire of CD4 T cells recognizing these epitopes, we sought to determine both the quantity and quality of the repertoire of insulin-reactive clones found in $Aire^{-/-}$, *Ins*-deficient ($Ins1^{-/-}Ins2^{-/-}B{:}16A^{tg+}$), and wild-type mice. $Ins1^{-/-}Ins2^{-/-}B{:}16A^{tg+}$ mouse lacks the expression of native insulin genes (*Ins1* and *Ins2*) and expresses a mutant form of *Ins2* with position InsB:16Y (Tyrosine) to A (Alanine) (B:16A), which effectively eliminates recognition by T cells, but provides endocrine insulin function (40). We immunized WT, $Aire^{-/-}$, and $Ins1^{-/-}Ins2^{-/-}B{:}16A^{tg+}$ mice with the immunogenic InsB:9-23 segment of insulin and 10 d later collected the draining lymph nodes to evaluate insulin-reactive T cells. We measured the number of IL-2-producing T cells by ELISPOT in response to a rechallenge with the full-length InsB:9-23 peptide or Reg3 mimotopes (Fig. 2*A*). Both $Aire^{-/-}$ and $Ins1^{-/-}Ins2^{-/-}B{:}16A^{tg+}$genotypes exhibited higher numbers of cells reactive against the full-length InsB:9-23 peptide. The $Ins1^{-/-}Ins2^{-/-}B{:}16A^{tg}$ mice had significantly higher IL-2-producing cells for both Reg3 mimotopes than WT mice. The $Aire^{-/-}$ mice showed higher numbers of IL-2-producing cells in Reg3 than WT mice, though a statistically significant increase was only found when insulin was presented in Reg3B. This suggests that in the absence of *Aire*- and *Ins*-expression, there is an increase in the quantity of insulin-reactive T cells that can escape thymic deletion and escape into the periphery.

Next, we sought to determine the quality of Reg3-specific insulin-reactive T cells in the $Aire^{-/-}$ and $Ins1^{-/-}Ins2^{-/-}B{:}16A^{tg}$ mice after immunization with InsB:9-23. Following immunization with InsB:9-23 peptide, register 3A-tetramer^{+} $CD4^{+}$ $CD44^{+}$ T cells were quantified by flow cytometry. We observed a significant increase in the frequencies and number of tetramer^{+} cells in the NOD.$Ins1^{-/-}Ins2^{-/-}B{:}16A^{tg}$ mice (Fig. 2*B*). We sorted these register 3A-tetramer^{+} CD4 T cells from pooled mice and used single-cell sequencing to identify their unique TCR alpha and beta chains. We obtained hundreds of paired TCR alpha and beta sequences in WT, *Ins*-deficient, and *Aire*-deficient genotypes for register 3A-tetramer^{+} cells (WT, n = 297; $Ins1^{-/-}Ins2^{-/-}B{:}16A^{tg}$, n = 384; $Aire^{-/-}$, n = 189) and fewer register 3B-specific cells (WT, n = 150; $Ins1^{-/-}Ins2^{-/-}B{:}16A^{tg}$, n = 33) (Fig. 2*C*). Clonal expansion within the dataset was assessed by matching all VDJ regions and CDR3 of both chains at the nucleotide level resulting in the identification of hundreds of unique clones (WT, n = 148; $Ins1^{-/-}Ins2^{-/-}B{:}16A^{tg}$, n = 146; $Aire^{-/-}$, n = 62) and fewer register 3B-specific cells (WT, n = 144; $Ins1^{-/-}Ins2^{-/-}B{:}16A^{tg}$, n = 30) (Fig. 2*C*). Considering only the unique clones identified, we observed a strong bias toward TRAV5D-4 gene usage across all three genotypes (Fig. 2*D* and *SI Appendix*, Figs. S2*A* and S3*A*), consistent with published literature highlighting the highly conserved TCR alpha chain

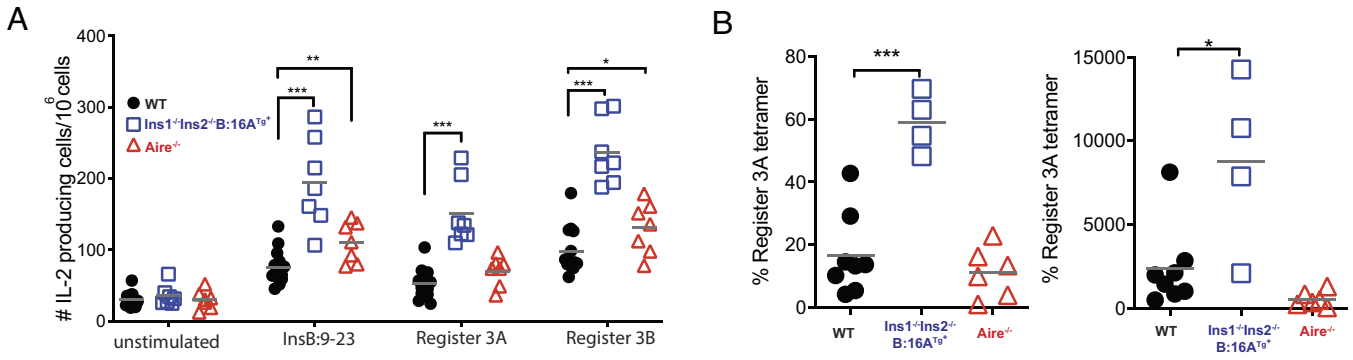

C

		WT	Ins1$^{-/-}$Ins2$^{-/-}$ B:16A^{Tg+}	Aire$^{-/-}$
Total single-cell TCRαβ paired sequences	Register 3A (p8E)	297	384	189
	Register 3B (p8G)	150	33	n/a
Unique TCRαβ paired sequences	Register 3A (p8E)	148	146	62
	Register 3B (p8G)	144	30	n/a

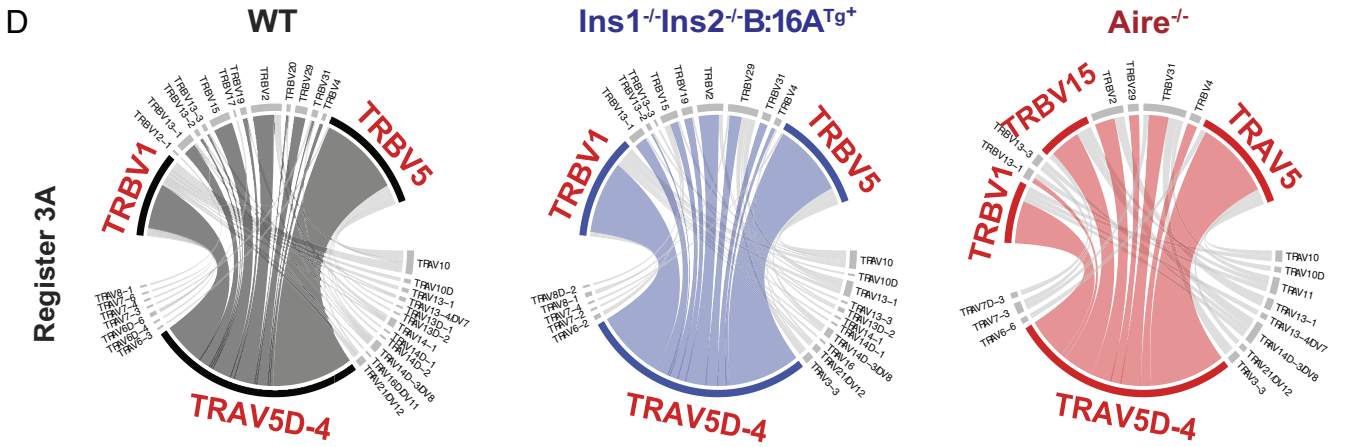

Fig. 2. *Aire*- and *Insulin*-dependent insulin-specific TCRs. NOD WT, *Aire*$^{-/-}$, and *Ins1*$^{-/-}$*Ins2*$^{-/-}$B:16A^{Tg+} mice were immunized with the immunogenic InsB:9-23, and the insulin-reactive clones were assessed after 10 d. (*A*) IL-2 ELIspot was used to enumerate the insulin-reactive clones in 1 × 10^6 cells via a rechallenge with the InsB:9-23, register 3A, and register 3B peptides. Experiments use 8 to 12-wk-old mice; male and female, n = 3. (*B*) Quantification of register 3A-reactive CD4$^+$ CD44$^+$ T cells in all three genetic backgrounds following immunization. This strategy was also used to isolate these Reg3A-reactive CD4$^+$ CD44$^+$ T cells for single-cell VDJ sequencing. (*C*) The table represents the total paired TCR sequences and the number of unique TCR clones recovered. (*D*) Circos plots depicting the frequency of TRAV-TRBV pairing within the unique clones identified across the three genotypes in the Reg3A-tetramer$^+$ cells. The dominant TRAV pairing with TRBV is colored for WT (black), Ins1$^{-/-}$Ins2$^{-/-}$B:16A^{Tg+} (blue), or *Aire*$^{-/-}$ (red) for clarity. 8 to 12-wk-old mice; male and female, n = 8 to 10 pooled/experiment). Data were analyzed by the unpaired *t* test and means shown in gray. Asterisks indicate significance determined between groups are *P < 0.05, **P < 0.01, ***P < 0.001, and ****P < 0.0001.

preference for insulin peptide recognition (25, 41, 42). A striking preference for TRBV1 and TRBV5 was observed across the three genotypes, in addition, *Aire*$^{-/-}$ genotype displayed a preference for TRBV15 (Fig. 2*D* and *SI Appendix*, Fig. S2*B*), suggesting that there may be some preferential beta chain gene usage in conjunction with the TRAV5D-4 bias. The Gini index was calculated to quantify the inequality of clonal distribution between the datasets ranging from 0 (maximum diversity, equal distribution of all clones) to 1 (no diversity, single clone) (43, 44). Although TCR alpha and beta gene usage were found to be similar across all three genotypes, there was an increase in the Gini index for the clones identified in *Ins1*$^{-/-}$*Ins2*$^{-/-}$*B:16A*^{tg} and *Aire*$^{-/-}$ mice compared to the WT mice, driven by the increased clonal expansion observed (>=2) (*SI Appendix*, Fig. S2*C* and Fig. 3*A*). Therefore, more gene usage restriction was observed within the clones in the *Ins1*$^{-/-}$*Ins2*$^{-/-}$*B:16A*^{tg} and *Aire*$^{-/-}$ insulin-reactive repertoires.

Next, we identified subsets of clones within the Reg3A dataset that were distinctive within the *Aire*$^{-/-}$ (n = 59), *Ins1*$^{-/-}$*Ins2*$^{-/-}$*B:16A*^{tg} (n = 140), or WT clonal datasets (n = 139) (*SI Appendix*, Fig. S2*D*). Here, a subset of TCRs' with matching VDJ gene usage and both CDR3 amino acid sequences were identified in both the WT and *Ins1*$^{-/-}$*Ins2*$^{-/-}$*B:16A*^{tg} insulin-reactive repertoires (n = 6), and WT and *Aire*$^{-/-}$ insulin-reactive repertoires (n = 3) (*SI Appendix*, Fig. S2*E*). However, no identical TCRs were shared across all three

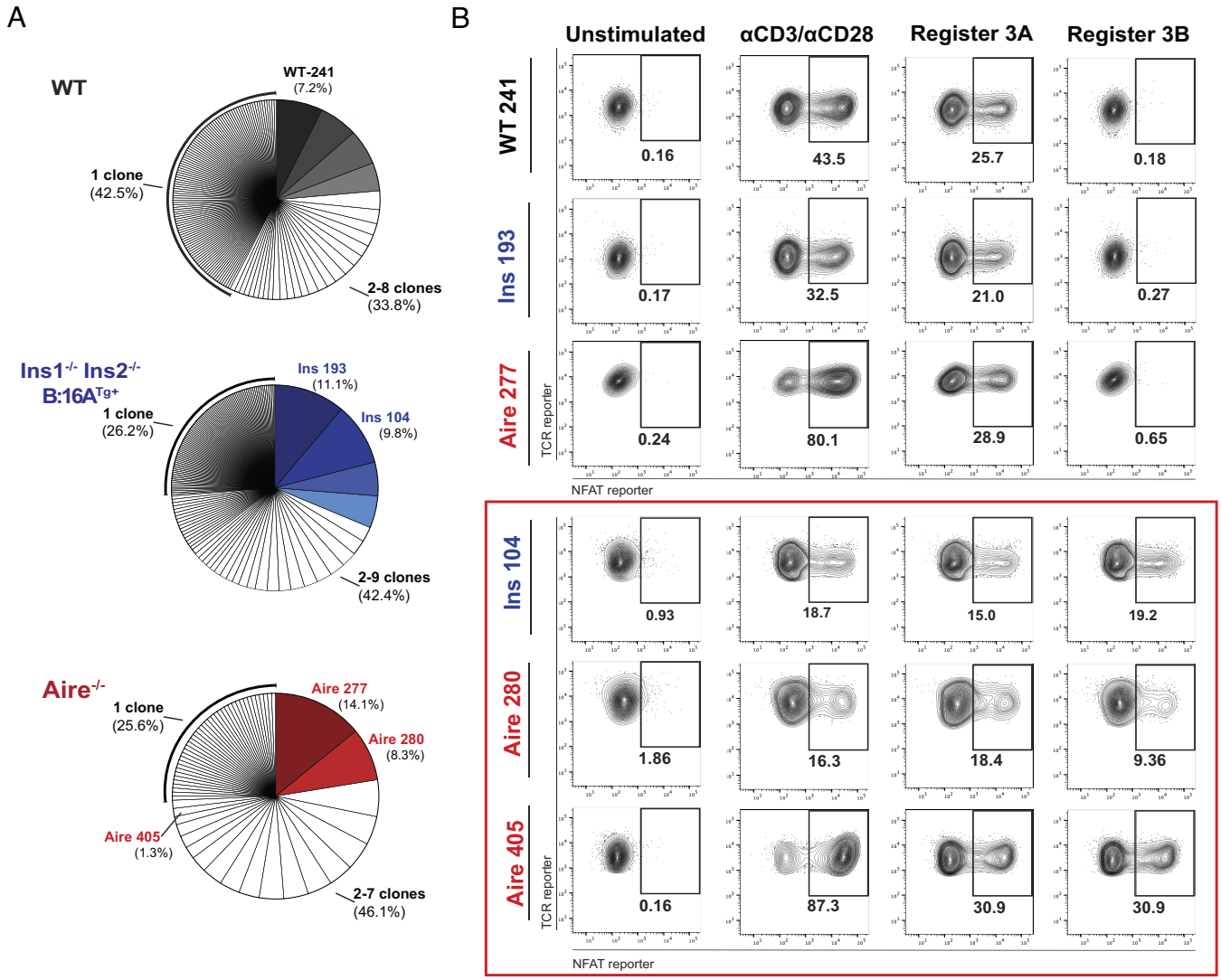

C

	TRAV	TRAJ	CDR3 Alpha	TRBV	TRBJ	TRBD	CDR3 Beta	Clonal expansion	%
Ins 104	TRAV5D-4	TRAJ18	CAASAG**GSALGRLHF**	TRBV1	TRBJ2-3	TRBD2	CTCSAT**GGG**AETLYF	37	9.81
Aire 280	TRAV5D-4	TRAJ18	CAASKG**GSALGRLHF**	TRBV1	TRBJ2-7	TRBD2	CTCSAD**GGG**AQEQYF	13	8.33
Aire 405	TRAV5D-4	TRAJ18	CAASAV**GSALGRLHF**	TRBV4	TRBJ1-2	TRBD2	CASSFTNSDYTF	2	1.28

Fig. 3. Identified tetramer$^+$ T cell clones are insulin reactive. The identified unique clones for each of the three genotypes were recreated into hybridomas expressing the NFAT-GFP reporter and were stimulated with plate-bound tetramers to confirm their reactivity in insulin. (*A*) Frequency of the unique TCR clones identified within each of the genotypes. TCRs of interest that were further investigated and their frequency out of all unique TCR sequences are shown. (*B*) Hybridomas were stimulated as described above for 20 to 24 h, and the GFP expression was assessed via Flow cytometry. Contour plots are shown, with numbers representing % of GFP$^+$ (NFAT$^+$) hybridomas out of all mCherry (TCR$^+$) cells. Representative plots of at least two independent experiments are shown. (*C*) Table displaying the gene usage of unique clones Ins-104, Aire-280, and Aire-405, highlighting shared CDR3 motifs between the clones.

genotypes. Comparing only the CDR3 alpha amino acid sequence, regardless of the VDJ gene usage, 10 CDR3 alpha sequences were shared between all three genotypes: the *Aire*$^{-/-}$ insulin-reactive repertoire shared 3 CDR3 alpha sequences with *Ins1*$^{-/-}$*Ins2*$^{-/-}$*B:16A*^{tg}, and 4 with the WT dataset, and the *Ins1*$^{-/-}$*Ins2*$^{-/-}$*B:16A*^{tg} insulin-reactive repertoire shared 13 with the WT dataset (*SI Appendix*, Fig. S2*F*). For CDR3 beta amino acid sequences, regardless of the VDJ usage, 5 were shared between all three genotypes, *Aire*$^{-/-}$ shared 2 sequences with *Ins1*$^{-/-}$*Ins2*$^{-/-}$*B:16A*^{tg} and 5 with WT; *Ins1*$^{-/-}$*Ins2*$^{-/-}$*B:16A*^{tg} shared 8 with WT (*SI Appendix*, Fig. S2*G*), suggesting public motifs within the CDR3 regions may contribute to the insulin recognition presented in Reg3A. These data did not reveal unique VDJ and CDR3 features associated with the Ins1$^{-/-}$Ins2$^{-/-}$B:16A^{tg} and Aire$^{-/-}$ datasets compared to the WT dataset; therefore, a signature of selection dependent on insulin expression in the thymus is not evident.

Similarly, we identified subsets of TCRs with the Reg3B dataset that are uniquely found in the *Ins1*$^{-/-}$*Ins2*$^{-/-}$*B:16A*^{tg} (n = 30) or in the WT mice (n = 141) (*SI Appendix*, Fig. S3*A*). A similar gene bias was found toward the TRAV5D-4 alpha chain (*SI Appendix*, Fig. S3*B*) and TRBV1 and TRBV5 beta chains. Pairing with TRBV2 gene usage was increased compared to Reg3

Type A TCRs (*SI Appendix*, Fig. S3 *A* and *B*). There were no shared TCRs between the genotypes (*SI Appendix*, Fig. S3*C*); however, there were 8 shared CDR3 alpha amino acid sequences, and 1 shared CDR3 beta amino acid sequence between the *Ins1*$^{-/-}$*Ins2*$^{-/-}$*B:16A*^{tg} and WT (*SI Appendix*, Fig. S3 *D* and *E*), suggesting again that there are public CDR3 motifs that contribute to insulin Reg3 Type B recognition. Several matching TCRs within the WT and *Ins1*$^{-/-}$*Ins2*$^{-/-}$*B:16A*^{tg} datasets were identified between the Reg3A and Reg3B datasets (*SI Appendix*, Fig. S3 *F* and *G*). This observation suggests that there are unique TCRs found with the WT and *Ins1*$^{-/-}$*Ins2*$^{-/-}$*B:16A*^{tg} datasets that may not fit into only the Reg3A and Reg3B categories and may be more promiscuous in their recognition of insulin. Furthermore, all the matched TCRs identified between the genotypes and Reg3A and RegB recognition utilize the TRAV5D-4 and either TRBV1/TRBV5 genes and are clonally expanded (=>2) within their respective datasets.

A Fraction of Clonally Expanded Reg3A-Binding Clones Cross-React with Insulin in Reg3B. We next sought to confirm the insulin reactivity of TCRs identified through sequencing. First, we identified the most frequent unique clones in each genotype WT-241 (7.2%), Ins-193 (11.1%), and Aire-227 (14.1%) (Fig. 3*A*). Additionally, we looked at several unique TCRs found in lower frequencies from the *Aire*$^{-/-}$ and *Ins1*$^{-/-}$*Ins2*$^{-/-}$*B:16A*^{tg} datasets Aire-280 (8.3%), Aire-405 (1.3%), and Ins-104 (9.8%) (Fig. 3*A*). These clones contained a CDR3 alpha "GSALGRLHF" motif found within the *Aire*$^{-/-}$ and *Ins1*$^{-/-}$*Ins2*$^{-/-}$*B:16A*^{tg} sequencing that was not within the WT insulin-reactive repertoires. Additionally, they differed in their TRBV gene usage and had unique CDR3 beta sequences (Fig. 3*B*). We utilized the in vitro retroviral expression system described previously (45) to rebuild these clones. Briefly, TCRs were introduced into expression vectors and retrovirally transduced into 58α^{-}β^{-}NFAT^{GFP} hybridoma lines, incubated with plate-bound Reg3A-tetramer or Reg3B-tetramers overnight, and analyzed for NFAT^{GFP} signaling. All TCRs identified and rebuilt responded to insulin presented in Reg3A, regardless of genotype (Fig. 3*C*). In addition, three of the tested TCRs also recognized insulin presented in Reg3B (Ins-104, Aire-280, and Aire-405). These cross-reactive TCRs all utilized the conserved TRAV5D-4 alpha chain. Ins-104 and Aire-280 share the CDR3 alpha motif "GSALGRLHF" and are paired with TRBV1 and share a CDR3 beta motif containing "GGGA" (Fig. 3*C*, bold). The Aire-405 TCR is distinctive, and although it contains a similar CDR3 alpha motif, "GSALGRLHF," it has a unique TRBV gene segment and CDR3 beta sequence. In sum, we identified several insulin-reactive clones that can respond to insulin presented in Reg3A and Reg3B that were found only in the *Aire*$^{-/-}$ and *Ins1*$^{-/-}$*Ins2*$^{-/-}$*B:16A*^{tg} datasets.

To further test the specificity of the dual reactive clones, we created a series of I-A^{g7} Reg3 mimotopes, substituting the p8 position with either the leucine (L) (Reg3-p8L) or valine (V) (Reg3-p8V). The Ins-104 and Aire-280 hybridomas responded only to the plate-bound Reg3A and Reg3B tetramers and not the Reg3-p8L or Reg3-p8V tetramers (Fig. 4*A*). In contrast, the Aire-405 clone responded robustly to all amino acid substitutions, suggesting that this TCR may have a promiscuous recognition of the presented peptide. The binding affinity of the Aire-405 TCR to the I-A^{g7} molecule presenting the range of register 3 peptides (Reg3A, Reg3B, and Reg3-p8V) was high, with a dissociation constant (KD, μM) calculated at 2.2, 3.0, and 11, respectively (Fig. 4*B*). These affinities are typical for conventional CD4 T cells with high affinity for conventional MHCII–foreign peptide complexes (46).

Next, we used Alanine screening to determine how the Aire-405 TCR interacts with the I-A^{g7} presenting the insulin peptide in Reg3A. Expression vectors encoding the Aire-405 TCR, control type A 12-4.1 TCR (47, 48), and control type B 8F10 TCR were transduced into the murine T cell (5KCα^{-}β^{-}) hybridoma cell line, which secretes IL-2 upon T cell stimulation. The relevant insulin mutant peptides were loaded onto M12.C3.G7 antigen-presenting cells, an I-A^{g7}-expressing variant of the B cell lymphoma, M12.C3 (33, 49), and cocultured with the TCR-expressing hybridomas for 24 h. The Aire-405 responded robustly to both the Reg3 WT (p9R) and Reg3A peptides (Reg3B was not included), whereas the control Reg3A and Reg3B clones only responded to the Reg3A and Reg3B peptides, respectively, but not well to the Reg3 WT (9R) insulin peptide (Fig. 4*C*). Mutating P-1 (-1A9E), P2 (2A9E), P3 (3A9E), and P5 (5A9E) Reg3A insulin peptide abolished the production of IL-2 from the 405-hybridoma (Fig. 4*C*), highlighting the importance of the N-terminal portion of the peptide in Aire-405 recognition. In sum, we identified a dual Reg3A+B reactive high-affinity TCR that recognizes insulin presented by the I-A^{g7} predominantly by the TCR alpha chain (TRAV and CDR3 regions) and is largely unaffected by alterations to the epitope in p8 position in the c-terminal region.

Insulin-Specific TCRs Identified from *Aire*-Deficient NOD Mice Can Evade Negative Selection in the Thymus. We next sought to determine whether the thymic selection of T cells expressing the Aire-405 and Aire-280 TCRs depended on *Ins* expression in the thymus. We first transduced the Aire-405 and Aire-280 TCR constructs into CD45.2^{+} Rag2$^{-/-}$ DN (double negative) thymocytes. These thymocytes were then introduced via intrathymic injection into the thymus of CD45.1^{+} WT or *Ins1*$^{-/-}$*Ins2*$^{-/-}$*B:16A*^{tg} mice that had been sublethally irradiated (*SI Appendix*, Fig. S4*A*). Thymocytes bearing the TCR of interest could be identified using a mCherry construct reporter and quantified via flow cytometry. We hypothesized that T cells sensitive to *Ins* expression in the thymus would be negatively selected during thymic development in WT animals but not in *Ins1*$^{-/-}$*Ins2*$^{-/-}$*B:16A*^{tg} mice. Indeed, significantly fewer CD4^{+} mCherry^{+} transduced cells were present in injected WT thymus when compared to *Ins1*$^{-/-}$*Ins2*$^{-/-}$*B:16A*^{tg} thymus (*SI Appendix*, Fig. S4*A*). No differences were found within the spleen (*SI Appendix*, Fig. S4*B*). Similar results were observed for the CD45.2^{+} expressing Aire-280 TCR, with significantly lower CD4^{+} mCherry^{+} cells in NOD.WT thymus and spleen when compared to NOD.*Ins1*$^{-/-}$*Ins2*$^{-/-}$*B:16A*^{tg} (*SI Appendix*, Fig. S4 *C* and *D*). These results support the conclusion that *Ins* expression in the thymus directly induces the negative selection of some insulin-reactive clones identified in mice deficient in *Aire*.

Next, we turned to a transgenic mouse system to test the thymic selection of the Aire-405 in the presence or absence of *Aire* and generated mice expressing the Aire-405 TCR (405^{Tg}) in the NOD background (50, 51). Here, we found evidence for robust expression of the 405 TCR in thymocytes (*SI Appendix*, Fig. S5*A*) and splenocytes (*SI Appendix*, Fig. S5*B*). The 405 TCR transgenic animals showed only minor differences in thymocyte frequencies compared to the NOD WT animals (*SI Appendix*, Fig. S5 *C* and *D*). We also noted a slight increase in CD5 expression on double-positive 405^{Tg} thymocytes and a slight decrease in CD5 expression on single-positive CD4^{+} thymocytes (*SI Appendix*, Fig. S5*E*) compared to NOD WT. 405^{Tg} animals had slightly lower amounts of FoxP3^{+} Tregs in the thymus (*SI Appendix*, Fig. S5*F*), a difference that was not observed in the periphery between 405^{Tg} and NOD WT animals (*SI Appendix*, Fig. S5*G*). The 405 TCR strongly binds to both Reg3A and Reg3B forms of insulin peptide (*SI Appendix*, Fig. S5*H*) in single-positive CD4^{+} thymocytes. Finally, when compared to NOD WT, 405^{Tg}

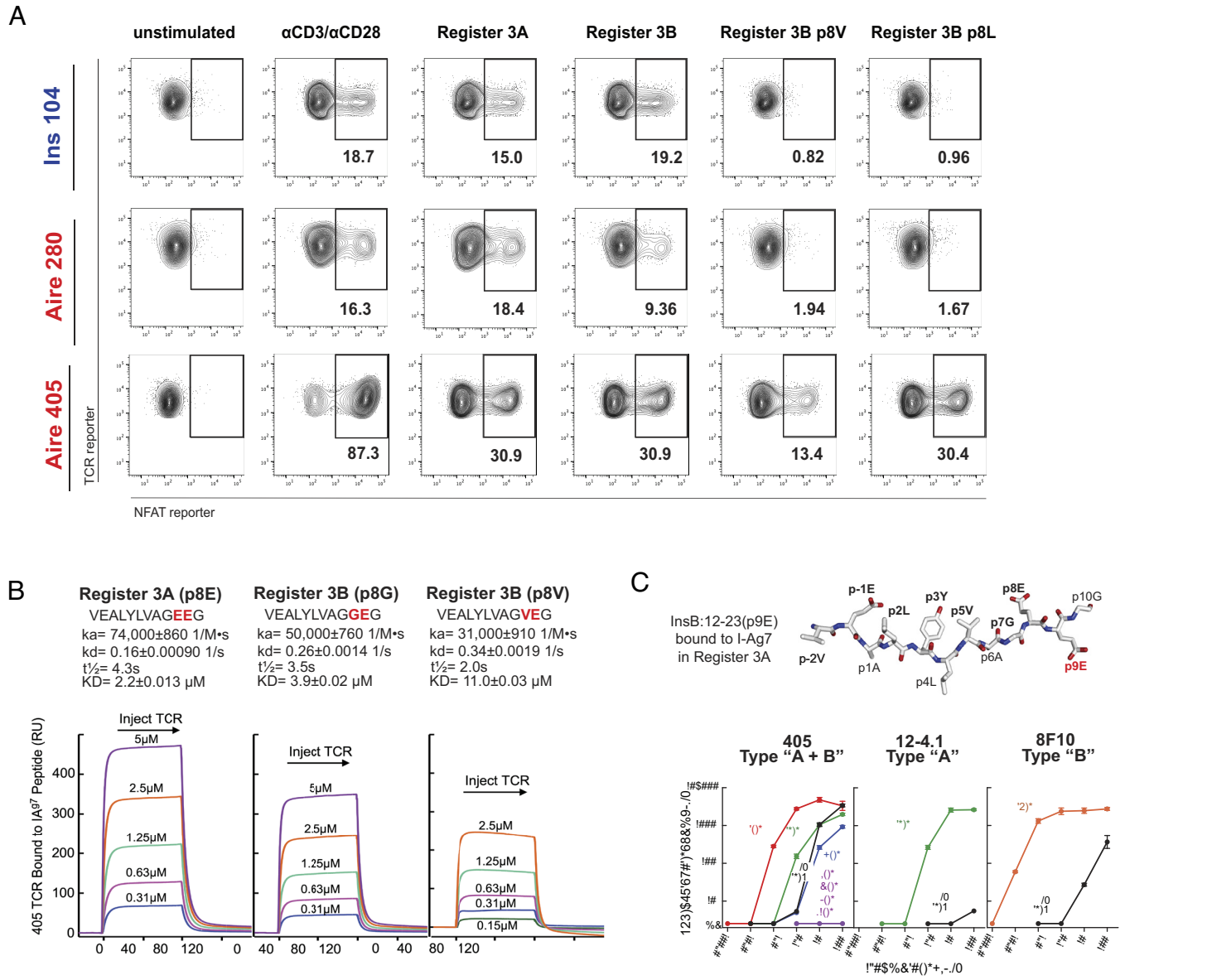

Fig. 4. Aire-405 TCR has promiscuous insulin recognition. (*A*) The Ins-104, Aire-280, and Aire-405 T cell hybridomas were stimulated with plate-bound tetramers to confirm their reactivity to the various register three peptides: p8E, p8G, p8V, and p8L. Hybridomas were stimulated as described above for 20 to 24 h, and the flow cytometry was used to access the % of GFP+ ($NFAT^+$) hybridomas out of all $mCherry^+$ (TCR^+) cells. Representative plots of at least two independent experiments are shown. (*B*) SPR data (RU, resonance units) from a single experiment are shown for binding of various concentrations of the soluble Aire-405 TCR to $I\text{-}A^{g7}$ with a covalent register three peptides bearing p8E, p8G, or p8V, each immobilized via a biotin tag in a BIAcore streptavidin flow cell. Data from a fourth flow cell containing immobilized $I\text{-}A^{g7}$–bound to a control peptide (HEL) was used to correct the fluid phase SPR signal data. Standard BIAcore Biaeval 4.0 software was used to fit the data to a first-order kinetic model and to calculate the kinetic association rate (kd, liters/mole s), dissociation rate (ka, 1/s), half-life (t½, s), and overall dissociation constant (KD, μM). Error bars represent SEMs. (*C*) Above: The structure of the InsB:12-23 peptide with the p9R>E mutation within the $I\text{-}A^{g7}$ groove is shown. Below: This soluble peptide (green) and versions with alanine mutations at upwardly pointing amino acids p-1, p2, p3, and p5 (violet), p7 (blue), and p8 (red) were titrated with $I\text{-}A^{g7}$ presenting cells to stimulate IL-2 production from the 5KC avatar T cell transduced with the 405 TCR. A version with natural unmutated p8Ep9R (black) was also used as a control peptide. The responses of a typical diabetic Type A (12-4.1) and Type B (8F10) T cell are shown with the p8Ep9R control peptide (black), and with a p9E peptide carrying the optimal p8 amino acid, E (12-4.1, green) or G (8F10, orange) are shown as well. The data are average with SEM of the normalized results of three separate experiments.

animals showed higher amounts of immune infiltrate, consistent with our model of 405 TCR as diabetogenic (*SI Appendix*, Fig. S5*I*).

To determine the effects of *Aire* deficiency on the clonal deletion of the 405^{Tg} transgenic cells, we next crossed 405^{Tg} mice to the $Aire^{-/-}$ genotype. Flow cytometry analysis of the thymus found no significant differences in overall thymic development (Fig. 5*A*). However, when the number of $V\beta10^+$ cells, the large majority of which express the transgenic TCR beta chain, was assessed within the SP $CD4^+$ T cells, a significant increase was found in $405^{Tg}Aire^{-/-}$ (84%) compared to the 405^{Tg} (75%) littermates (Fig. 5*B*). Moreover, a greater increase in Reg3A-reactive $tetramer^+$ cells was also seen (43% 405^{Tg}; 74% $405^{Tg}Aire^{-/-}$) (Fig. 5*C*). We also found a dramatic decrease in the number of $Vb10^+$ Tregs ($FoxP3^+$ CD25hi) in the thymus of 405^{Tg} $Aire^{-/-}$ compared to the 405^{Tg} controls (Fig. 5*D*). In the periphery, we did not observe a difference in the percentage of CD4 T cells nor $V\beta10^+$ cells (Fig. 5 *E* and *F*). However, an increase in the percentage of high-affinity Reg3A-reactive $tetramer^+$ cells was found (Fig. 5*G*), as these cells appear to be more persistent in the periphery. In addition, insulitis dramatically increased in the $405^{Tg}Aire^{-/-}$ at 12 wk of age (Fig. 5*H*) compared to the 405^{Tg} mice; however, we did not find mice spontaneously developing diabetes in this background similar to what

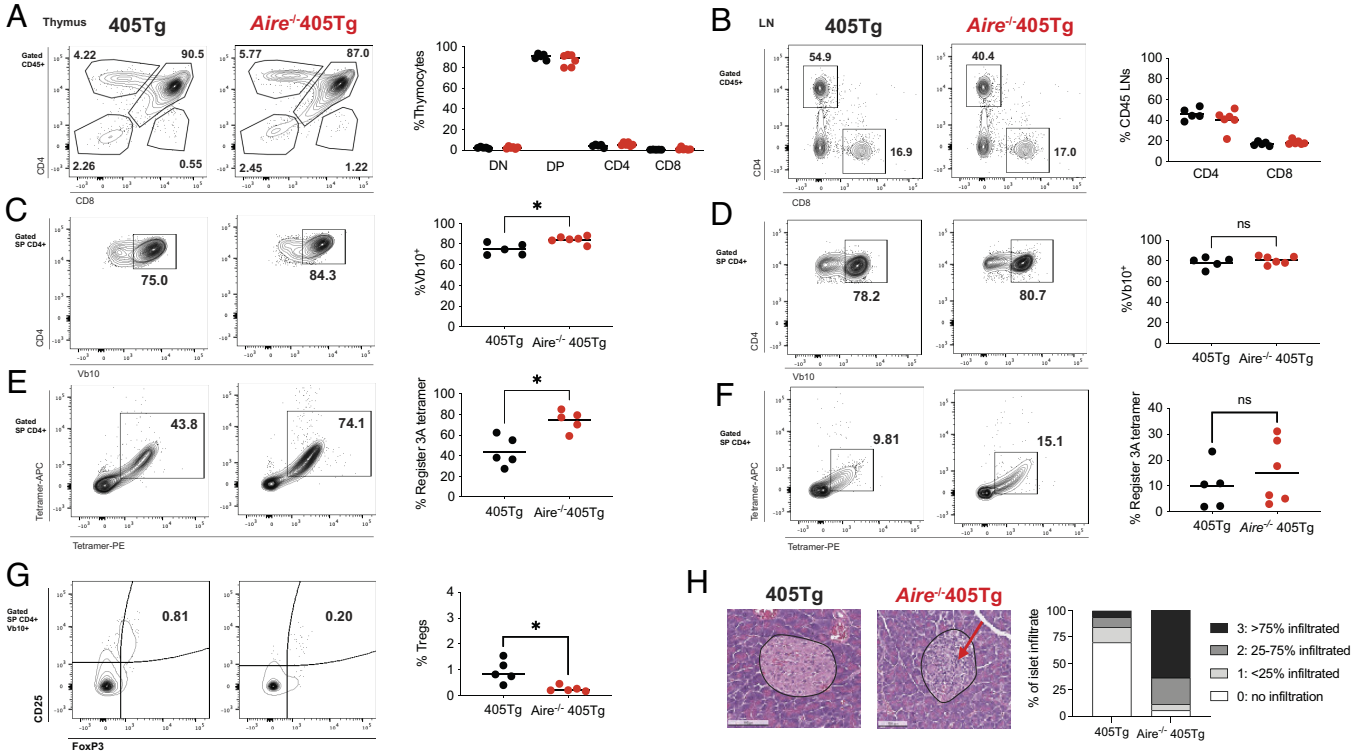

Fig. 5. Insulin-specific T cell clone 405 undergoes Aire-mediated deletion. (*A*) CD4 and CD8 flow cytometric profiles of 405^{Tg} and $Aire^{-/-}405^{Tg}$ thymocytes (*Left*). Percentage of DN (double negative), DP (double positive), SP (single positive) CD4, and SP CD8 thymocytes (*Right*). (*B*) Representative plots of cell surface staining of $V\beta10^{+}$on SP CD4 T cells in the periphery (*Left*). Percentage of $V\beta10^{+}$ SP CD4 T cells in the periphery (*Right*). (*C*) Representative plots of double positive (APC and PE) Reg3A-tetramer staining of SP CD4 T cells thymocytes (*Left*). Percentage of $Tetramer^{+}$ SP CD4 T cells thymocytes (*Right*). (*D*) FoxP3 staining of SP CD4 cells thymocytes (*Left*). Percentages of $FoxP3^{+}$ $CD25^{hi}$ in the WT and 405^{Tg} mice (*Right*). (*E*) CD4 and CD8 flow cytometric profiles of 405^{Tg} and $Aire^{-/-}405^{Tg}$ in the periphery (pooled LNs) (*Left*). Percentage of CD4 and CD8 T cells (out of total $CD45^{+}$ cells) in the periphery (*Right*). (*F*) Representative plots of cell surface staining of $V\beta10^{+}$on SP CD4 thymocytes (*Left*). Percentage of $V\beta10^{+}$ SP CD4 thymocytes (*Right*). (*G*) Representative plots of double positive (APC and PE) low and high-affinity Reg3A-tetramer staining of SP CD4 T cells in the periphery (*Left*). Percentage of low and high-affinity Reg3A-$tetramer^{+}$ SP CD4 T cells in the periphery (*Right*). (*H*) Significant peri-islet lymphocytic infiltrate (red arrows) on islet histology of $Aire^{-/-}405^{Tg}$ mice (*Left*). A dramatic increase in the insulitis levels in the $Aire^{-/-}405^{Tg}$ mice compared to 405^{Tg} controls is also observed at 12 wk (males and females), consistent with reduced deletion of these autoreactive cells (*Right*). Data were analyzed by the unpaired *t* test, and the mean was displayed. Asterisks indicate significance $*P < 0.05$.

has been described for other islet-specific TCR transgenic lines (52, 53).

Discussion

Here, we have identified Aire-405 TCR, a unique high-affinity clone for InsB:9-23 bound in $I\text{-}A^{g7}$ in the unfavorable Reg3 that is nonetheless deleted in the thymus via *Aire*-dependent mechanisms. Despite the existing knowledge of the thymic expression of insulin in both humans and mice, limited studies have directly examined the selection of insulin-specific cells in the thymus. In addition, it is important to emphasize that previous investigations of specific insulin-reactive TCRs have utilized clones derived from *Aire*-sufficient hosts and, therefore, were less likely to identify specificities that are dependent on *Aire*-driven expression of thymic insulin. The identification of Aire-405 TCR underscores the significance of examining not just the TCR sequences and their in vitro and in vivo properties but also emphasizes the crucial role of the genetic background from which they originate.

Insulin-specific CD4 T cells in NOD mice are generally restricted to a dominant peptide epitope, InsB:9-23, that can be presented by $I\text{-}A^{g7}$ in three different registers (29, 30, 34, 54, 55). Previous work by Unanue et al. proposed two epitopes within the InsB:9-23, creating two sets of insulin-reactive T cells referred to as type A and B (35, 36, 38, 39). Meanwhile, Kappler et al. demonstrated that most InsB:9-23 T cell clones identified in NOD mice recognize insulin in register three stabilized by the introduction of glutamic acid (E) at position nine replacing the unfavorable arginine R (32, 33, 55). Selection of the insulin-reactive clones in the thymus has been proposed by both Kappler and Unanue groups to be associated with weak-peptide binding and with the poorly presented epitopes capable of escaping deletion (Type B and register 3B) in comparison to their stably presented counterparts which results in deletion or Treg selection (Type A and register 3A). Unlike previous studies that measured cell frequencies in the periphery (38), we developed TCR transgenic mouse lines to directly assess the thymic selection of both types of canonical T cells. Here, we find that when this method directly assesses thymic selection, neither a canonical Reg3A clone (4F7) nor a canonical Reg3B clone (8F10) had their thymic selection altered in the absence of *Aire*.

As the canonical Reg3A and Reg3B reactive clones, 4F7 and 8F10, were identified in an *Aire*-sufficient host, we reasoned that insulin-reactive clones dependent on *Aire*-expression in the thymus are more likely to be identified in the mice deficient for *Aire*. Utilizing the register 3 tetramers, our sequencing results identified important consistencies across the three genotypes including the preferential use of the TRAV5D-4 gene for the TCR alpha chain consistent with published data (41). Uniquely, we identified a consistent preference in the use of the TCR beta chain within the dataset of insulin-reactive TCRs, regardless of the genotype. This dataset is valuable for researchers studying insulin-specific CD4 T cells in the NOD mouse

model. Further investigation into the uniquely identified and expanded clones in the *Aire*-deficient genotype highlighted clones that were cross-reactive to both register 3 conformations (Reg3A and Reg3B). Intriguingly, these data suggest that TCRs with this property could have enough c-terminal promiscuity to react against an insulin-hybrid peptide which has been recently invoked as an important potential trigger for T1D (56). Ultimately, the establishment of the TCR transgenic model for Aire-405 allowed us to directly assess how *Aire* and thymic insulin expression influence the selection of high-affinity T cells. Notably, we observed reduced deletion of this TCR in the *Aire*-deficient background, concomitant with a decrease in thymic Foxp3$^+$ Tregs in the *Aire*-deficient background, implying that thymic insulin plays a role in driving their positive selection. These results demonstrate that the thymic expression of insulin through Aire drives thymic selection against high-affinity insulin-specific TCRs. However, low-affinity TCRs can pass through this mechanism relatively unscathed, and this may also be related to the relatively weak binding of the dominant insulin epitope for CD4 T cells of InsB:9-23.

Our results support a model by which thymic insulin expression driven by *Aire* is important for trimming high-affinity T cells, and these results suggest that perhaps developing alternative approaches to enhance or stabilize insulin expression in the thymus could be explored to enhance tolerance in T1D. For example, introducing stabilized *Ins* register 3 epitopes into the thymus may enhance central tolerance mechanisms. Another potential option is to increase the levels of *Aire* expressing mTECs within the thymus, increasing the levels of *Ins* expression. We have previously shown that OPG$^{-/-}$ mice dramatically increase the number of Aire$^+$ mTECs (57), highlighting the importance of the RANK-RANKL-OPG axis. Whether selectively blocking the decoy receptor for RANKL, OPG, or treatment with RANK-Fc would lead to increased mTECs. Another approach may include using embryonic stem cell-derived thymic epithelial cells (21) to generate a new functional thymus that can be engineered to express the stabilized insulin. Such approaches are now becoming feasible and could help translate our fundamental findings here on thymic selection to changing the course of immune tolerance to insulin and the development of T1D.

Materials and Methods

Mice. Female NOD/ShiLtJ (Jackson laboratories) mice were housed and bred under specific pathogen-free conditions in accordance with the UCSF (San Francisco, CA) Animal Care and Use Committee guidelines. NOD. 8F10^{Tg} and NOD.4F7Tg mice have been previously described (36, 37). *Aire*$^{-/-}$ NOD mice were maintained in the lab. *Ins1*$^{-/-}$*Ins2*$^{-/-}$*B:16A*$^{tg+}$transgenic line NOD mice were a gift from Maki Nakayama (University of Colorado Denver). All protocols were approved by the UCSF Institutional Animal Care and Use Committee.

Hybridoma Assays. TCRs of interest were cloned into the pMSCV-IRES-mCherry retroviral vector (Addgene). The virus was generated using Phoenix-ECO packaging cells to transduce the TCR-deficient 58$\alpha^-\beta^-$ hybridoma cell line, modified to express GFP downstream of an NFAT promoter. Hybridomas were stimulated with 2.5 μg/mL plate-bound tetramer) in PBS coated for 2 h at 37 °C (33). Cells were stimulated and analyzed the following day for GFP expression.

Flow Cytometry. Single-cell suspensions from various organs were blocked with tetramer block (2.4G2, BioXcel, Normal Rat Serum, Jackson Immunoresearch. Thomas Scientific) and stained with antibodies of indicated specificities in PBS buffer with 2% FBS. APC- or PE-conjugated tetramer of I-A^{g7} bound to insulin 9:23 mimotopes p8E (HLVERLYLVCGEEG) and p8G (HLVERLYLVCGGEG) (33) and HEL (AMKRHGLDNYRGYSL), obtained from the NIH tetramer facility, Atlanta, GA. Flow cytometry analyses were performed on an LSRII (BD Biosciences) and were analyzed with Flow Jo software (TreeStar, Inc.). For additional details, see *SI Appendix, Supplemental Experimental Procedures*.

Immunization. Mice were immunized in the flank with 0.1 mg of peptide (GeneScript) emulsified 1:1 in Complete Freund's Adjuvant (7001, Chondrex). Cells were collected for downstream analysis 10 d later.

IL-2-Specific Enzyme-Linked ImmunoSpot Assay. Enzyme-Linked ImmunoSpot (ELISPOT) assays in MultiScreen 96-well plates (S2EM004M99, Millipore) were performed according to manufacturer guidelines using the BD ELISPOT Mouse IL-2 ELISPOT Pair (551876, BD Biosciences). Plates were developed by incubating with 1:500 with streptavidin-HRP (557630; BD Biosciences) for 1 h at room temperature and developed using AEC Substrate and AEC Chromogen (551951, BD Biosciences). Plates were dried until image capture and spot counting by a CTL ELISpot reader with Immunospot software. Data are presented as "cSPW" (background-subtracted "Corrected Spots/Well").

Tetramer Pull-Down Enrichment. Tetramer enrichment and staining were performed as previously described (58, 59). CD3$^+$CD4$^+$CD8$^-$CD44$^+$Tetramer$^+$ cells were FACs sorted on a FACs Aria 3u (BD Biosciences).

Single-Cell TCRαβ Sort and Sequencing. Tetramer$^+$cells were flow sorted into single wells of a 96-well plate, and TCR sequences were obtained using three rounds of PCR to amplify and barcode before sequencing on an Illumina MiSeq. For additional details, see *SI Appendix, Supplemental Experimental Procedures*.

Soluble Peptides and I-A^{g7}-Peptide Complexes. All soluble peptides for these studies were obtained from GenScript Biotech Corp and used as described in the text. For the InsB:9-23 insulin peptides, various truncations and mutations were used, as described in the test for individual experiments. In most in vitro experiments with these soluble peptides, the cysteine at B:19 was mutated to alanine to avoid peptide dimerization. Biotinylated soluble versions of I-A^{g7} complexed with peptide were produced either in the NIH Tetramer Core Facility for flow cytometry experiments or in the Kappler laboratory (32, 33) for surface plasmon resonance (SPR) experiments as described. For additional details, see *SI Appendix, Supplemental Experimental Procedures*.

SPR Measurements. Approximately 2,000 RU of biotinylated I-A^{g7}-8E9E, I-A^{g7}-8G9E, I-A^{g7}-8L9E, or I-A^{g7} with a HEL control peptide were captured in the four separate flow cells of a BIAcore streptavidin BIAsensor chip. Various concentrations of the soluble 405 TCR were injected, and the association and dissociation kinetics were followed by recording the SPR signal. The SPR data were analyzed with BIAcore BIAEval 4 software using the signal obtained with the control I-A^{g7}-HEL flow cell to correct for the fluid phase resonance signal.

Generation of Aire-405 TCR Transgenic Mice. Transgenic mice were produced by the Mouse genetic core facility at National Jewish Health. The TCR variable region of the Aire-405 alpha chain was cloned into the pCD2 vector, and the beta chain was cloned into the p428 TCR transgenic vector (50, 51). Plasmids were linearized and co-injected into NOD embryos. More details are included in *SI Appendix* section.

Histology. Pancreas were harvested and fixed overnight in 10% formalin, washed in 30% ethanol, and then stored in 70% ethanol. The fixed pancreas was embedded in paraffin, sectioned, and stained with H&E by HistoWiz, Inc. Scoring of immune infiltration was performed blind.

Statistical Analysis. Unless stated otherwise, analysis was performed using Prism 9 (GraphPad Software). All statistical tests performed and *P*-values are stated in the figure legends.

Data, Materials, and Software Availability. Raw short-read sequences for this project have been deposited in the Sequence Read Archive (SRA) and assigned the bioproject number PRJNA1082731(60). The datasets generated during the current study are available in Dataset S1.

ACKNOWLEDGMENTS. We thank Anderson, Bluestone, and Kappler laboratory members for their technical support and discussions. We thank Wei Dong Wu for his assistance with mouse maintenance and technical support.

We thank the members of the University of California San Francisco Flow Cytometry Core Facility for their assistance. This work was supported by National Institute of Allergy and Infectious Disease P01 (AI118688) National Institute of Diabetes and Digestive and Kidney Diseases R01 (DK133443) the Larry L. Hillblom Foundation. J.A.S. and W.P. were supported partly by the Larry L. Hillblom Foundation Diabetes Fellowship (2019-D-006-FEL & 2013-D-006-FEL). B.T.K.Y. was supported by the Juvenile Diabetes Research Foundation Fellowship (3-PDF-2017-401-A-N).

Author affiliations: [a]Diabetes Center, University of California San Francisco, San Francisco, CA 94143; [b]Department of Immunology and Genomic Medicine, National Jewish Health, Denver, CO 80206; [c]Sean N. Parker Autoimmune Research Laboratory, Diabetes Center, University of California, San Francisco, CA 94143; [d]Barbara Davis Center for Diabetes, University of Colorado Anschutz Medical Campus, Aurora, CO 80045; and [e]Department of Immunology and Microbiology, University of Colorado Anschutz Medical Campus, Aurora, CO 80045

Author contributions: J.A.S., B.T.K.Y., W.P., F.C., J.A.B., J.W.K., and M.S.A. designed research; J.A.S., B.T.K.Y., W.P., J.M.B., J.D.P., F.C., and J.W.K. performed research; F.C. contributed new reagents/analytic tools; J.A.S. and B.T.K.Y. analyzed data; and J.A.S., B.T.K.Y., J.M.B., J.W.K., and M.S.A. wrote the paper.

1. L. T. Jeker, H. Bour-Jordan, J. A. Bluestone, Breakdown in peripheral tolerance in type 1 diabetes in mice and humans. *Cold Spring Harb. Perspect. Med.* **2**, a007807 (2012).
2. M. S. Anderson, J. A. Bluestone, The NOD mouse: A model of immune dysregulation. *Annu. Rev. Immunol.* **23**, 447–485 (2005).
3. S. M. Lieberman, T. P. DiLorenzo, A comprehensive guide to antibody and T-cell responses in type 1 diabetes. *Tissue Antigens* **62**, 359–377 (2003).
4. L. Zhang, M. Nakayama, G. S. Eisenbarth, Insulin as an autoantigen in NOD/human diabetes. *Curr. Opin. Immunol.* **20**, 111–118 (2008).
5. M. Nakayama *et al.*, Prime role for an insulin epitope in the development of type 1 diabetes in NOD mice. *Nature* **435**, 220–223 (2005).
6. D. Hanahan, Peripheral-antigen-expressing cells in thymic medulla: Factors in self-tolerance and autoimmunity. *Curr. Opin. Immunol.* **10**, 656–662 (1998).
7. S. T. Bennett *et al.*, Insulin VNTR allele-specific effect in type 1 diabetes depends on identity of untransmitted paternal allele. The IMDIAB Group. *Nat. Genet.* **17**, 350–352 (1997).
8. A. Pugliese *et al.*, The insulin gene is transcribed in the human thymus and transcription levels correlated with allelic variation at the INS VNTR-IDDM2 susceptibility locus for type 1 diabetes. *Nat. Genet.* **15**, 293–297 (1997).
9. I. Durinovic-Belló *et al.*, Class III alleles at the insulin VNTR polymorphism are associated with regulatory T-cell responses to proinsulin epitopes in HLA-DR4, DQ8 individuals. *Diabetes* **54** (suppl. 2), S18 (2005).
10. I. Durinovic-Belló *et al.*, Insulin gene VNTR genotype associates with frequency and phenotype of the autoimmune response to proinsulin. *Genes Immun.* **11**, 188–193 (2010).
11. P. Vafiadis *et al.*, Insulin expression in human thymus is modulated by INS VNTR alleles at the IDDM2 locus. *Nat. Genet.* **15**, 289–292 (1997).
12. M. S. Anderson *et al.*, Projection of an immunological self shadow within the thymus by the aire protein. *Science* **298**, 1395–1401 (2002).
13. Finnish-German APECED Consortium, An autoimmune disease, APECED, caused by mutations in a novel gene featuring two PHD-type zinc-finger domains. *Nat. Genet.* **17**, 399–403 (1997).
14. K. Nagamine *et al.*, Positional cloning of the APECED gene. *Nat. Genet.* **17**, 393–398 (1997).
15. F. Cetani *et al.*, A novel mutation of the autoimmune regulator gene in an Italian kindred with autoimmune polyendocrinopathy-candidiasis-ectodermal dystrophy, acting in a dominant fashion and strongly cosegregating with hypothyroid autoimmune thyroiditis. *J. Clin. Endocrinol. Metab.* **86**, 4747–4752 (2001).
16. M. A. Su *et al.*, Mechanisms of an autoimmunity syndrome in mice caused by a dominant mutation in Aire. *J. Clin. Invest.* **118**, 1712–1726 (2008).
17. B. E. Oftedal *et al.*, Dominant mutations in the autoimmune regulator AIRE are associated with common organ-specific autoimmune diseases. *Immunity* **42**, 1185–1196 (2015).
18. S. N. Sansom *et al.*, Population and single-cell genomics reveal the Aire dependency, relief from Polycomb silencing, and distribution of self-antigen expression in thymic epithelia. *Genome Res.* **24**, 1918–1931 (2014).
19. P. Brennecke *et al.*, Single-cell transcriptome analysis reveals coordinated ectopic gene-expression patterns in medullary thymic epithelial cells. *Nat. Immunol.* **16**, 933–941 (2015).
20. M. Meredith, D. Zemmour, D. Mathis, C. Benoist, Aire controls gene expression in the thymic epithelium with ordered stochasticity. *Nat. Immunol.* **16**, 942–949 (2015).
21. J. L. Bautista *et al.*, Single-cell transcriptional profiling of human thymic stroma uncovers novel cellular heterogeneity in the thymic medulla. *Nat. Commun.* **12**, 1096 (2021).
22. N. C. Schloot, S. Willemen, G. Duinkerken, R. R. de Vries, B. O. Roep, Cloned T cells from a recent onset IDDM patient reactive with insulin B-chain. *J. Autoimmun.* **11**, 169–175 (1998).
23. G. Semana, R. Gausling, R. A. Jackson, D. A. Hafler, T cell autoreactivity to proinsulin epitopes in diabetic patients and healthy subjects. *J. Autoimmun.* **12**, 259–267 (1999).
24. D. K. Cole *et al.*, Hotspot autoimmune T cell receptor binding underlies pathogen and insulin peptide cross-reactivity. *J. Clin. Invest.* **126**, 3626 (2016).
25. D. R. Wegmann, M. Norbury-Glaser, D. Daniel, Insulin-specific T cells are a predominant component of islet infiltrates in pre-diabetic NOD mice. *Eur. J. Immunol.* **24**, 1853–1857 (1994).
26. D. R. Wegmann, R. G. Gill, M. Norbury-Glaser, N. Schloot, D. Daniel, Analysis of the spontaneous T cell response to insulin in NOD mice. *J. Autoimmun.* **7**, 833–843 (1994).
27. D. Zekzer *et al.*, Inhibition of diabetes by an insulin-reactive CD4 T-cell clone in the nonobese diabetic mouse. *Diabetes* **46**, 1124–1132 (1997).
28. F. S. Wong *et al.*, Identification of an MHC class I-restricted autoantigen in type 1 diabetes by screening an organ-specific cDNA library. *Nat. Med.* **5**, 1026–1031 (1999).
29. D. Daniel, R. G. Gill, N. Schloot, D. Wegmann, Epitope specificity, cytokine production profile and diabetogenic activity of insulin-specific T cell clones isolated from NOD mice. *Eur. J. Immunol.* **25**, 1056–1062 (1995).
30. N. Abiru *et al.*, Dual overlapping peptides recognized by insulin peptide B:9–23 T cell receptor AV13S3 T cell clones of the NOD mouse. *J. Autoimmun.* **14**, 231–237 (2000).
31. F. Crawford, E. Huseby, J. White, P. Marrack, J. W. Kappler, Mimotopes for alloreactive and conventional T cells in a peptide–MHC display library. *PLoS Biol.* **2**, e90 (2004).
32. F. Crawford, H. Kozono, J. White, P. Marrack, J. Kappler, Detection of antigen-specific T cells with multivalent soluble class II MHC covalent peptide complexes. *Immunity* **8**, 675–682 (1998).
33. F. Crawford *et al.*, Specificity and detection of insulin-reactive CD4+ T cells in type 1 diabetes in the nonobese diabetic (NOD) mouse. *Proc. Natl. Acad. Sci. U.S.A.* **108**, 16729–16734 (2011).
34. M. G. Levisetti, A. Suri, S. J. Petzold, E. R. Unanue, The insulin-specific T cells of nonobese diabetic mice recognize a weak MHC-binding segment in more than one form. *J. Immunol.* **178**, 6051–6057 (2007).
35. J. F. Mohan, S. J. Petzold, E. R. Unanue, Register shifting of an insulin peptide-MHC complex allows diabetogenic T cells to escape thymic deletion. *J. Exp. Med.* **208**, 2375–2383 (2011).
36. J. F. Mohan, B. Calderon, M. S. Anderson, E. R. Unanue, Pathogenic CD4+ T cells recognizing an unstable peptide of insulin are directly recruited into islets bypassing local lymph nodes. *J. Exp. Med.* **210**, 2403–2414 (2013).
37. X. Wan *et al.*, Pancreatic islets communicate with lymphoid tissues via exocytosis of insulin peptides. *Nature* **560**, 107–111 (2018).
38. J. F. Mohan *et al.*, Unique autoreactive T cells recognize insulin peptides generated within the islets of Langerhans in autoimmune diabetes. *Nat. Immunol.* **11**, 350–354 (2010).
39. J. F. Mohan, E. R. Unanue, Unconventional recognition of peptides by T cells and the implications for autoimmunity. *Nat. Rev. Immunol.* **12**, 721–728 (2012).
40. M. Nakayama *et al.*, Establishment of native insulin-negative NOD mice and the methodology to distinguish specific insulin knockout genotypes and a B:16 alanine preproinsulin transgene. *Ann. N. Y. Acad. Sci.* **1037**, 193–198 (2004).
41. M. Nakayama *et al.*, Germline TRAV5D-4 T-cell receptor sequence targets a primary insulin peptide of NOD mice. *Diabetes* **61**, 857–865 (2012).
42. L. Zhang *et al.*, Analysis of T cell receptor beta chains that combine with dominant conserved TRAV5D-4*04 anti-insulin B:9–23 alpha chains. *J. Autoimmun.* **33**, 42–49 (2009).
43. V. Sadras, R. Bongiovanni, Use of Lorenz curves and Gini coefficients to assess yield inequality within paddocks. *Field Crops Res.* **90**, 303–310 (2004).
44. P. G. Thomas, A. Handel, P. C. Doherty, N. L. La Gruta, Ecological analysis of antigen-specific CTL repertoires defines the relationship between naïve and immune T-cell populations. *Proc. Natl. Acad. Sci. U.S.A.* **110**, 1839–1844 (2013).
45. A. Spence *et al.*, Revealing the specificity of regulatory T cells in murine autoimmune diabetes. *Proc. Natl. Acad. Sci. U.S.A.* **115**, 5265–5270 (2018).
46. Y. Wang *et al.*, C-terminal modification of the insulin B:11–23 peptide creates superagonists in mouse and human type 1 diabetes. *Proc. Natl. Acad. Sci. U.S.A.* **115**, 162–167 (2018).
47. J. M. Jasinski *et al.*, Transgenic insulin (B:9–23) T-cell receptor mice develop autoimmune diabetes dependent upon RAG genotype, H-2g7 homozygosity, and insulin 2 gene knockout. *Diabetes* **55**, 1978–1984 (2006).
48. E. Simone *et al.*, T cell receptor restriction of diabetogenic autoimmune NOD T cells. *Proc. Natl. Acad. Sci. U.S.A.* **94**, 2518–2521 (1997).
49. E. Carrasco-Marin, J. Shimizu, O. Kanagawa, E. R. Unanue, The class II MHC I-Ag7 molecules from non-obese diabetic mice are poor peptide binders. *J. Immunol.* **156**, 450 (1996).
50. Q. Wang *et al.*, CD4 promotes breadth in the TCR repertoire. *J. Immunol.* **167**, 4311–4320 (2001).
51. T. Zhumabekov, P. Corbella, M. Tolaini, D. Kioussis, Improved version of a human CD2 minigene based vector for T cell-specific expression in transgenic mice. *J. Immunol. Methods* **185**, 133–140 (1995).
52. A. Gonzalez *et al.*, Genetic control of diabetes progression. *Immunity* **7**, 873–883 (1997).
53. J. D. Katz, B. Wang, K. Haskins, C. Benoist, D. Mathis, Following a diabetogenic T cell from genesis through pathogenesis. *Cell* **74**, 1089–1100 (1993).
54. A. R. Burton *et al.*, On the pathogenicity of autoantigen-specific T-cell receptors. *Diabetes* **57**, 1321–1330 (2008).
55. B. D. Stadinski *et al.*, Diabetogenic T cells recognize insulin bound to IAg7; in an unexpected, weakly binding register. *Proc. Natl. Acad. Sci. U.S.A.* **107**, 10978 (2010).
56. R. L. Baker, B. L. Jamison, K. Haskins, Hybrid insulin peptides are neo-epitopes for CD4 T cells in autoimmune diabetes. *Curr. Opin. Endocrinol. Diabetes Obes.* **26**, 195–200 (2019).
57. I. S. Khan *et al.*, Enhancement of an anti-tumor immune response by transient blockade of central T cell tolerance. *J. Exp. Med.* **211**, 761–768 (2014).
58. D. I. Kotov, M. K. Jenkins, Peptide:MHCII tetramer-based cell enrichment for the study of epitope-specific CD4+ T cells. *Curr. Protoc. Immunol.* **125**, e75 (2019).
59. H. H. Chu *et al.*, Positive selection optimizes the number and function of MHCII-restricted CD4+ T cell clones in the naive polyclonal repertoire. *Proc. Natl. Acad. Sci. U.S.A.* **106**, 11241–11245 (2009).
60. J. Smith, M. Anderson, Data from "Insulin-specific T cell sequencing." TCR raw sequence reads. NIH. http://www.ncbi.nlm.nih.gov/bioproject/PRJNA1082731. Deposited 1 March 2024.